ACTA ENTOMOLOGICA
MUSEI NATIONALIS PRAGAE
ISSN 1804-6487 (online) – 0374-1036 (print)

2024
64(2): 269–276
doi: 10.37520/aemnp.2024.018
www.aemnp.eu

RESEARCH PAPER

A new species of *Autocrates* (Coleoptera: Trictenotomidae) revealed by DNA barcoding and morphological evidence

Hee-Wook CHO[1)] & Kang-Rae KIM[2)]

[1)] Nakdonggang National Institute of Biological Resources, Sangju 37242, South Korea; e-mail: lampides@gmail.com
[2)] Southeast Sea Fisheries Research Institute, National Institute of Fisheries Science, Namhae 52440, South Korea; e-mail: krkim89@korea.kr

Accepted:
28th September 2024

Published online:
31st October 2024

Abstract. *Autocrates soni* sp. nov. is described from Vietnam based on morphological and molecular evidence. This beetle is characterised by reddish-brown pubescence on its ventral side and much shorter setae on its femora compared to the closely related species *Autocrates vitalisi* Vuillet, 1912. The validity of this new species is strongly supported by DNA barcode data from all known species of the genus *Autocrates*.

Key words. Coleoptera, Tenebrionoidea, Trictenotomidae, *Autocrates*, new species, DNA barcoding, phylogeny, Vietnam, Oriental Region

Zoobank: http://zoobank.org/urn:lsid:zoobank.org:pub:E373C5E4-AD21-407C-9AB6-F69984FA1CDB

Introduction

The family Trictenotomidae Blanchard, 1845, is a small group of beetles currently containing 18 species in 2 genera: *Autocrates* Thomson, 1860, with 6 species and *Trictenotoma* Gray, 1832, with 12 species (Hu et al. 2022). This group is widely distributed in the Oriental Region extending to the south of the Palaearctic Region of China, and is also known from South Korea. Trictenotomid beetles are remarkable for their large and robust adults resembling some members of two unrelated families, Lucanidae and Cerambycidae. However, the placement of this unique family within the superfamily Tenebrionoidea is clearly supported by larval and adult morphology, molecular data and bionomics (e.g., McKenna et al. 2019, Cho et al. 2022). Members of *Autocrates* are very similar in their external morphology as well as male genitalia and terminalia (Hu et al. 2022). Therefore, species identification is highly dependent on other characters (e.g., colouration, male mandible shape, density of setae). However, it is unclear whether such differences in external characters represent interspecific differences. Specimens of *Autocrates vitalisi* Vuillet, 1912, from Khanh Vinh, Vietnam, show reddish-brown pubescence on the ventral surface that is not found in other areas, while there are no significant differences in male or female genitalia between regions.

DNA barcoding typically uses standardised sequences of the mitochondrial cytochrome *c* oxidase subunit I (COI) region for species identification (Hebert et al. 2003). This method shows remarkable accuracy and reproducibility compared to traditional morphological taxonomic methods that struggle to match different life cycle stages and dimorphic sexes, and also allows for differentiating between closely related species (Antil et al. 2023, Chen et al. 2024). Nevertheless, identification based on DNA barcodes should be supported by other evidence, particularly morphology (Meier et al. 2024). A recent study highlighted the clear molecular distinction between species belonging to the genus *Autocrates* (Lee et al. 2024).

In the present study, we found that individuals seemingly belonging to *A. vitalisi* from Khanh Vinh, Vietnam, in fact represent a new species, as phylogenetic analysis using DNA barcode sequences placed them into a different clade. Photographs of the habitus, terminalia and genitalia of the new species, diagnostic characters and a key to the species of *Autocrates* are provided.

Material and methods

Morphological analysis. Adults of *Autocrates soni* sp. nov. were collected by light traps (150-watt black light bulb) at Son Thai (12°11′26.5″N, 108°43′03.5″E) in Khanh Hoa Province, South Central Vietnam (Figs 1A–D). Specimens were examined under a Leica S8APO microscope (Leica Microsystems, Wetzlar, Germany). Dry specimens were softened in a plastic box with wet tissue paper for 12 hours; subsequently, the abdomen was dissected at its lateroapical margin and genitalia extracted using forceps.

Male and female genital segments were cleaned in 10% (w/v) sodium hydroxide and rinsed in distilled water. Photographs of external morphology were taken using a Nikon D7500 digital camera fitted with a 60 mm lens (Nikon, Tokyo, Japan), while photographs of the genital segments were obtained using a Nikon D750 digital camera attached to a Leica S8APO microscope. The images were stacked using Helicon Focus image stacking software and digitally edited. The morphological terminology follows Hu et al. (2022). Body length was measured from the tip of the mandible to the apex of the elytra and body width was measured at the greatest width of the elytra. The type series of the new species has been deposited in the collections of the National Museum of the Czech Republic, Prague (NMPC), Mancheon Insect Museum, Seoul, South Korea (MIM) and H. W. Cho's private collection (HCC).

DNA extraction, sequencing and phylogenetic analysis. The abdominal tissue samples were preserved in 99% ethanol. Then, genomic DNA was extracted from the preserved tissues of all specimens using DNeasy Blood & Tissue Kit (QIAGEN, Germantown, MD, USA) in accordance with the manufacturer's protocol. The primers for mitochondrial DNA (mtDNA) were sourced from a previous study (LCO1490: GGTCAACAAATCATAAAGATATTGG; HCO2198: TAAACTTCAGGGTGACCAAAAAATCA) and PCR was carried out using AccuPower® Multiplex PCR Premix Kit (BIONEER Co., Daejeon, South Korea) on a Mastercycler® Pro Gene Amplifier (Eppendorf, Hamburg, Germany). The 20 µl reaction mixtures contained 1 µl genomic DNA, 1 µl each

Table 1. Details of the partial COI sequences used in the phylogenetic analysis.

Taxon	Locality	Accession No.	Remarks
Trictenotoma davidi	China: Fujian, Longyan	OP324567	Cho et al. (2022)
T. davidi	China: Fujian, Longyan	OP324568	Cho et al. (2022)
T. pollocki	Vietnam: Binh Thuan, Dong Tien	PQ360854	
Autocrates aeneus	China: Tibet, Nyingchi	OQ709433	Lee et al. (2024)
A. aeneus	China: Tibet, Nyingchi	OQ709434	Lee et al. (2024)
A. aeneus	China: Tibet, Nyingchi	OQ709435	Lee et al. (2024)
A. ivanovi	Vietnam: Lam Dong, Da Lat	PQ358386	
A. ivanovi	Vietnam: Kon Tum, Dak Glei	OQ709431	Lee et al. (2024)
A. lini	China: Guangxi, Xiangzhou	OQ709438	Lee et al. (2024)
A. maqueti	South Korea: Uljin	PQ360857	
A. maqueti	South Korea: Uljin	PQ358391	
A. oberthueri	China: Yunnan, Weixi Lisu	OP324565	Cho et al. (2022)
A. oberthueri	China: Yunnan, Weixi Lisu	OP324566	Cho et al. (2022)
A. oberthueri	China: Yunnan, Weixi Lisu	OQ709428	Lee et al. (2024)
A. oberthueri	China: Yunnan, Weixi Lisu	OQ709429	Lee et al. (2024)
A. oberthueri	China: Yunnan, Weixi Lisu	OQ709430	Lee et al. (2024)
A. soni sp. nov.	Vietnam: Khanh Hoa, Khanh Vinh	PQ360855	
A. soni sp. nov.	Vietnam: Khanh Hoa, Khanh Vinh	PQ360856	
A. soni sp. nov.	Vietnam: Khanh Hoa, Khanh Vinh	PQ360858	
A. vitalisi	Vietnam: Yen Bai	PQ358393	
A. vitalisi	Vietnam: Yen Bai	PQ358395	
A. vitalisi	Vietnam: Kon Tum	PQ358398	
A. vitalisi	China: Yunnan, Yingjiang	OQ709436	Lee et al. (2024)
A. vitalisi	China: Yunnan, Hani and Lahu	OQ709437	Lee et al. (2024)

forward and reverse primer (1.0 mM) and 17 µl distilled water. The PCR cycling conditions consisted of an initial denaturation step at 95°C for 2 min followed by 35 cycles of denaturation at 94°C for 30 s, annealing at 52°C for 30 s and extension at 72°C for 30 sec, and a final extension step at 72°C for 10 min; the reaction was terminated at 4°C. The amplified COI fragments were sequenced using an ABI 3730xl DNA Analyzer (Applied Biosystems, Foster City, CA, USA). Phylogenetic tree was constructed in MEGA using maximum likelihood with 1000 bootstrap replicates. To determine genetic divergence, we used the *p*-distance method in MEGA

Results

Molecular phylogenetic analysis based on mitochondrial COI gene

Amplification products consisting of 658 bp of the mitochondrial COI gene were successfully obtained from 10 individuals belonging to 5 species. Comparative species sequences were retrieved from GenBank for available species of the family Trictenotomidae (Table 1). Maximum likelihood phylogenetic inferences based on the COI gene are shown in Fig. 2. Each clade showed strong grouping with conspecifics within the genus *Autocrates*. *Autocrates soni* sp. nov. was closely related to *Autocrates lini* Hu, Drumont & Telnov, 2022, but differences in branch length suggested that the clades diverged earlier. Analysis of *p*-distance within the genus *Autocrates* showed a range of 0.085 to 0.163 indicating that nucleotide sequence differences between species ranged from 8.5% to 16.3% (Table 2). The *p*-distance range between the species of the genus *Autocrates* and *A. soni* sp. nov. was 8.5% to 16%, indicating a species-level difference. *Autocrates soni* sp. nov. showed the smallest nucleotide sequence differences from *A. vitalisi* and *A. lini* (8.5% and 8.7%, respectively).

Taxonomy

Autocrates soni sp. nov.

(Figs 3–5)

Type locality. Vietnam, Khanh Hoa Province, Khanh Vinh District, Son Thai, 12°11′26.5″N, 108°43′03.5″E, 1,604 m a.s.l.

Type material. Holotype: ♂ (NMPC), "Vietnam, Khanh Hoa Province, Khanh Vinh District, Son Thai, 12°11′26.5″N 108°43′03.5″E, v.2020, local collector leg.", plus red holotype label. Paratypes: 3 ♂♂ 4 ♀♀ (MIM), same data as holotype, plus red paratype label; 4 ♂♂ 6 ♀♀ (MIM), same data as holotype except viii.2020; 1 ♂ 1 ♀ (HCC), same data as holotype except vi.2022; 1 ♀ (NMPC), same data as holotype except v.2023; 1 ♀ (HCC), same data as holotype except vi.2023; 1 ♂ 1 ♀ (MIM), same data as holotype except 16.vi.2023, T. W. Kim leg.

Description. *General appearance* (Figs 3A–E). Body length 54.0–76.5 mm, width 21.0–27.5 mm, elongate-oval

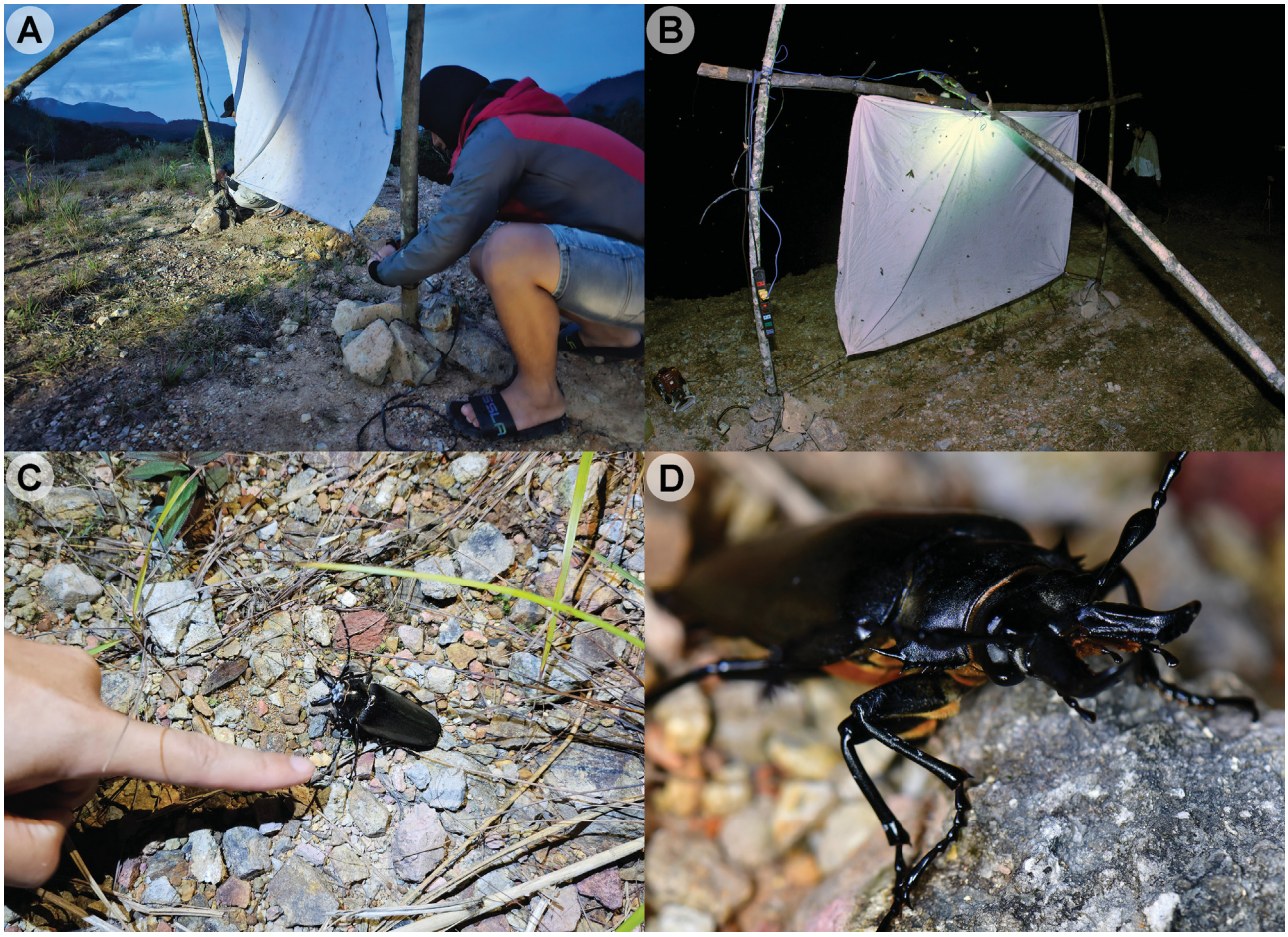

Fig. 1. Type locality of *Autocrates soni* sp. nov. A–B – light equipment used for collecting; C–D – living individuals attracted by light (photographed by Min-Woo Son).

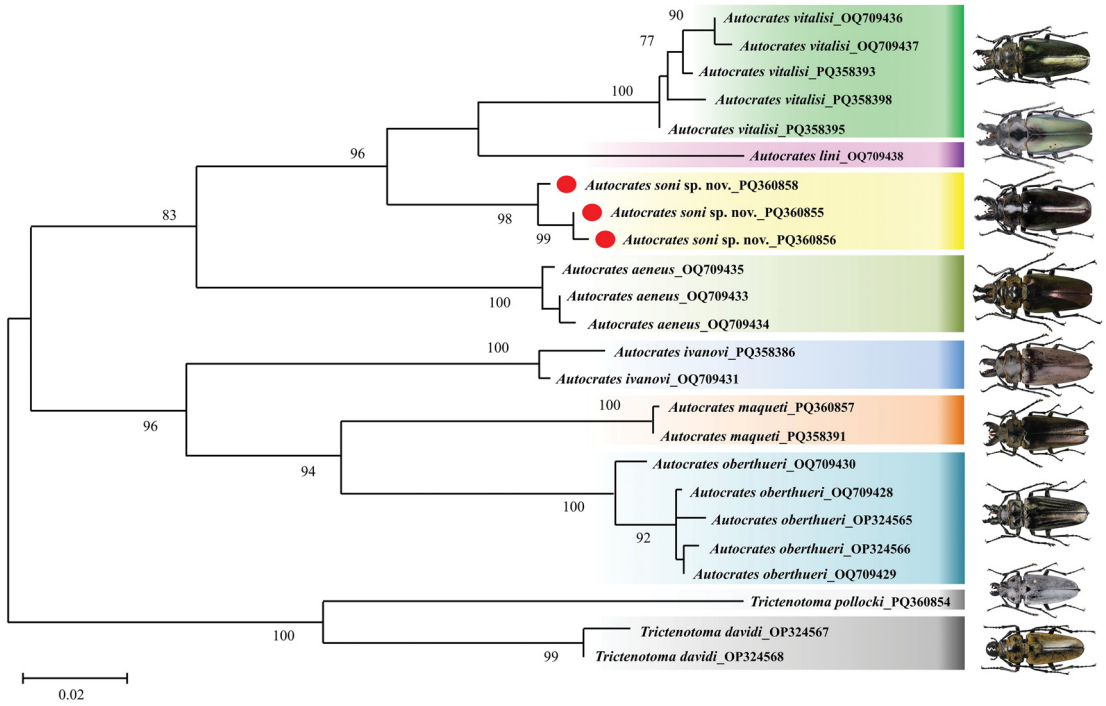

Fig. 2. Maximum likelihood tree of all species of *Autocrates* Thomson, 1860 based on COI sequences.

and dorsoventrally flattened. Ground colour uniformly black with weak metallic lustre. Dorsum entirely covered with dense, short, appressed, yellow to ochre pubescence; venter laterally covered with dense, rather long, reddish-brown pubescence.

Head prognathous, transverse, distinctly narrower than pronotum. Frons slightly impressed, declivous. Clypeus weakly emarginate along anterior margin. Labrum strongly transverse, broadly emarginate, with setose anterior margin. Compound eyes moderately large, strongly vertically oriented and narrow. Mentum sparsely covered with long setae. Hypopharynx densely covered with long setae. Mandible enlarged, apex unidentate, with strongly asymmetric inner teeth; apical half of male mandible distinctly bent upwards, particularly in large males. Apical maxillary palpomere narrowly securiform, slightly longer than penultimate palpomere. Genal ridges produced anteriad and apically subacute in male, more strongly produced and apically acute to subacute in female. Male antennae much longer than half body length; antennomere I (scapus) largest, longest, distinctly widened distally; II (pedicellus) short; III–VIII elongate, each subequal in length; VIII with distinct lateral projection on distal part; IX–X flabellate; XI lanceolate. Female antennae less than half body length; antennomere VIII with shorter lateral projection in distal part.

Thorax. Pronotum transverse, about twice as wide as long, anterolateral angle strongly obtusely produced, posterolateral angle with short spine. Lateral margin of pronotum with 6–8 acute spines; largest spine directed obliquely backwards, situated in posterior 1/3. Pronotal disc densely punctulate, decumbently setose. Prosternal intercoxal process glabrous, finely and sparsely punctulate. Meso- and metaventrite with meson largely glabrous.

Table 2. Sequence divergence determined using *p*-distance in MEGA.

	A. aeneus	***A. ivanovi***	***A. lini***	***A. maqueti***	***A. soni* sp. nov.**	***A. oberthueri***	***A. vitalisi***
A. aeneus	-						
A. ivanovi	0.152	-					
A. lini	0.128	0.163	-				
A. maqueti	0.163	0.134	0.175	-			
A. soni sp. nov.	0.111	0.137	0.087	0.160	-		
A. oberthueri	0.159	0.130	0.156	0.113	0.145	-	
A. vitalisi	0.122	0.136	0.082	0.163	0.085	0.137	-

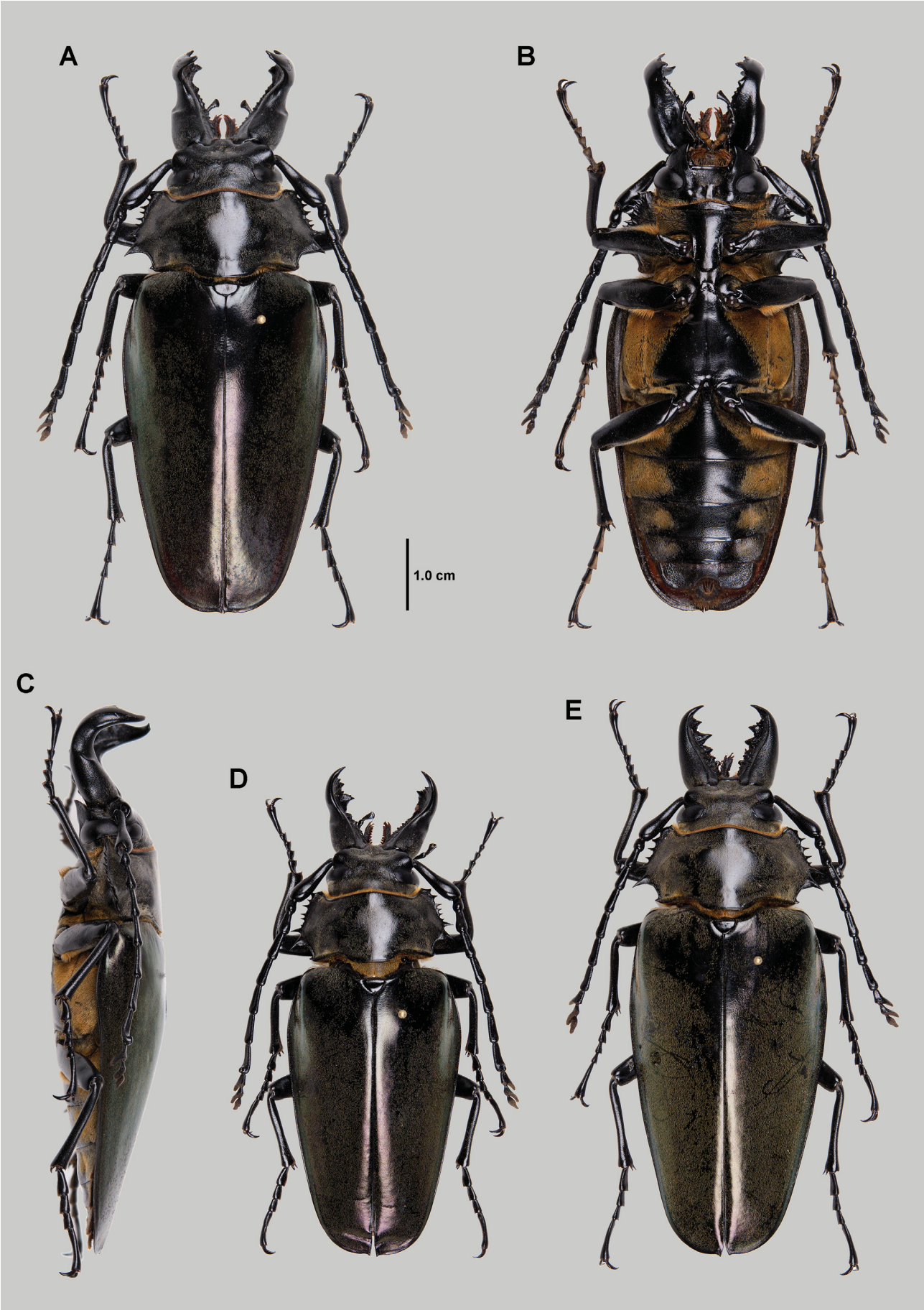

Fig. 3. Habitus of *Autocrates soni* sp. nov. A–C – holotype. A – male, dorsal view; B – male, ventral view; C – male, lateral view. D–E – paratypes. D – male, dorsal view; E – female, dorsal view

Scutellum slightly wider than long, narrowed posteriorly.

Elytra, hind wings and femora. Lateral sides moderately widened posteriorly up to basal 1/4, thence gradually narrowed posteriorly. Elytral apices not meeting at suture, each armed with short angulate tooth. Humeral calli broadly rounded. Disc densely punctulate, decumbently setose. Hind wings well developed. Femora covered with sparse punctures bearing short setae with row of brush-like, dense setae at inner margin.

Abdomen. Each abdominal ventrite nearly glabrous along midline. Basale of aedeagus broad; apicale elongate, slender and apically tapering, with two short apical processes; pair of accessory lobes long and narrow extending beyond apex of apicale, with spatulate and setose distal part (Figs 4A–B). Male sternite VII deeply U-shaped emarginate. Male tergite VII narrowed apically, posterior margin broadly emarginate, densely setose (Fig. 4C). Male tergite VIII shallowly emarginate on posterior margin, surface densely setose (Fig. 4D). Male sternite VIII strongly bilobed, posterior margin deeply emarginate and densely setose, with pair of long and slender protrusions on lateral margin (Fig. 4E). Male tergites IX and X fused, elongate oval and membranous (Figs 4F–G). Female tergites VII–VIII and sternite VIII as in Figs 4H and I. Ovipositor very long and slender, with short gonostyli.

Differential diagnosis. *Autocrates soni* sp. nov. is almost identical to *A*. *vitalisi* Vuillet, 1912, in its general appearance and genital structure. However, the new species can be distinguished by the reddish-brown pubescence on the ventral side as shown in Fig. 5A (yellow, ochre to ochre-greyish in *A*. *vitalisi* as in Fig. 5B); femora except inner margin covered with sparse punctures bearing short setae (much longer setae in *A*. *vitalisi*); dorsum black with very weak metallic lustre (dorsum generally cupreous, purple or pale green metallic in *A*. *vitalisi*). *Autocrates lini* Hu, Drumont & Telnov, 2022, is also similar, but differs in the golden pubescence on venter and glabrous dorsum.

Etymology. This new species is dedicated to Mr. Hyunsu Son (Hwaseong, South Korea), an amateur beetle collector who first pointed out the morphological differences of this new species.

Distribution. Vietnam: Khanh Hoa.

Discussion

Members of *Autocrates* show a high degree of similarity in their external morphology. According to the key to *Autocrates* species provided by Hu et al. (2022), accurate identification is generally possible based only on large males because females and smaller males are more uniform in appearance. The shape of male genitalia, often used as a key diagnostic character for distinguishing species, is almost identical between closely related species within the genus. Therefore, other characters (body colouration, shape of male mandible, colour and density of setae, etc.) are used to identify the species of the genus *Autocrates*.

However, it is unclear whether such differences in external features are inter- or intraspecific. This limitation can be effectively addressed using DNA barcoding markers, which can distinguish not only adults but also larvae and eggs. Notably, species of *Autocrates* are ideal candidates for taxa that are difficult to differentiate by traditional morphological identification. This study demonstrated that species of *Autocrates* can be classified by the 658 bp COI region. The difficulty of species delimitation based on morphology was overcome by discovering a new species through DNA barcoding. Genetic distance thresholds for insect species identification are typically between 2% and 5%, but thresholds varied among taxa, e.g., 9.18% for most species of entiminine weevils (Ma et al. 2022). *Autocrates soni* sp. nov. has a sequence difference of 8–16%, which is consistent with the species-level difference, and was therefore determined to be a new species. Interestingly, this new species is closely related to *A. lini* and *A*. *vitalisi*, but the branch length suggests an early divergence time. These ancient divergences can be identified through molecular barcoding, providing insights into species divergence and identification of potential new species. Therefore, DNA barcoding markers are highly effective molecular indicators for identifying new species, making them especially valuable for recognising new or potential species within the genus *Autocrates*.

Key to the species of the genus *Autocrates*

(modified from Hu et al. 2022, suitable for large males)

1 Apical half of male mandible strongly bent upwards (up to 90°); most lateral spines of pronotum prominent, long and acutely pointed; lateral margins of pronotum diverging gradually from anterolateral angles towards largest lateral spine. 2
– Male mandible parallel to body axis or bent slightly upwards at apex only; lateral spines of pronotum comparatively short, denticle-like with only largest, prebasal, lateral spine long and strongly prominent; lateral margins of pronotum subparallel or broadly rounded, not gradually diverging posteriad. 4
2 Most of pronotum and elytron glabrous, pronotal and elytral setae, if present, minute, inconspicuous and sparse; dorsum generally black with green lustre, distinctly stronger on elytra compared to forebody (China). ..... ***A. lini*** Hu, Drumont & Telnov, 2022
– Dorsum densely covered with short setae; dorsum generally black, cupreous, purple or pale green metallic, but without bright green lustre on elytra. 3
3 Venter with reddish-brown setae; femora except inner margin covered with sparse punctures bearing much shorter setae (Vietnam: Khanh Hoa). ..... ***A. soni* sp. nov.**
– Venter with ochre to ochre-greyish setae; femora except inner margin covered with sparse punctures bearing much longer setae (Cambodia, China, Laos, Malaysia, Myanmar, Thailand, Vietnam). ..... ***A. vitalisi*** Vuillet, 1912
4 Male mandible bent outwards around midlength, provided with wide and high dorsal carina; lateral margin of pronotum slightly dentate, (sub)parallel in front of largest lateral spine; largest lateral pronotal spine

generally straight, rarely curved (Bhutan, China, India, Myanmar, Nepal). ..... ***A. aeneus*** (Westwood, 1846)

– Male mandible on same axis as body, not bent outwards and not carinate dorsally; lateral margin of pronotum slightly dentate, at least weakly rounded in front of largest lateral spine; largest lateral spine generally curved posteriad, rarely nearly straight. 5

5 Elytron with several longitudinal rows of greyish to ochre-greyish setae; lateral margin of pronotum distinctly rounded; basal half of male mandible distinctly swollen dorsally (China). .... ***A. oberthueri*** Vuillet, 1910

– Elytron uniformly pale brown to greyish setose; lateral margin of pronotum weakly rounded, either straight; male mandible not swollen dorsally in basal half or (only in large males) slightly swollen laterally. 6

6 Distal half of outer margin of male mandibles hollowed out; base of pronotum across posterolateral angles nearly same width as elytra across base; elytral setation whitish to greyish (Vietnam). .... ***A. ivanovi*** Drumont, 2016

– Distal half of outer margin in male mandibles flat, not hollowed out; base of pronotum across posterolateral angles distinctly narrower than elytra across base; elytral setation ochre to ochre-brown (China, Korea). ..... ***A. maqueti*** Drumont, 2006

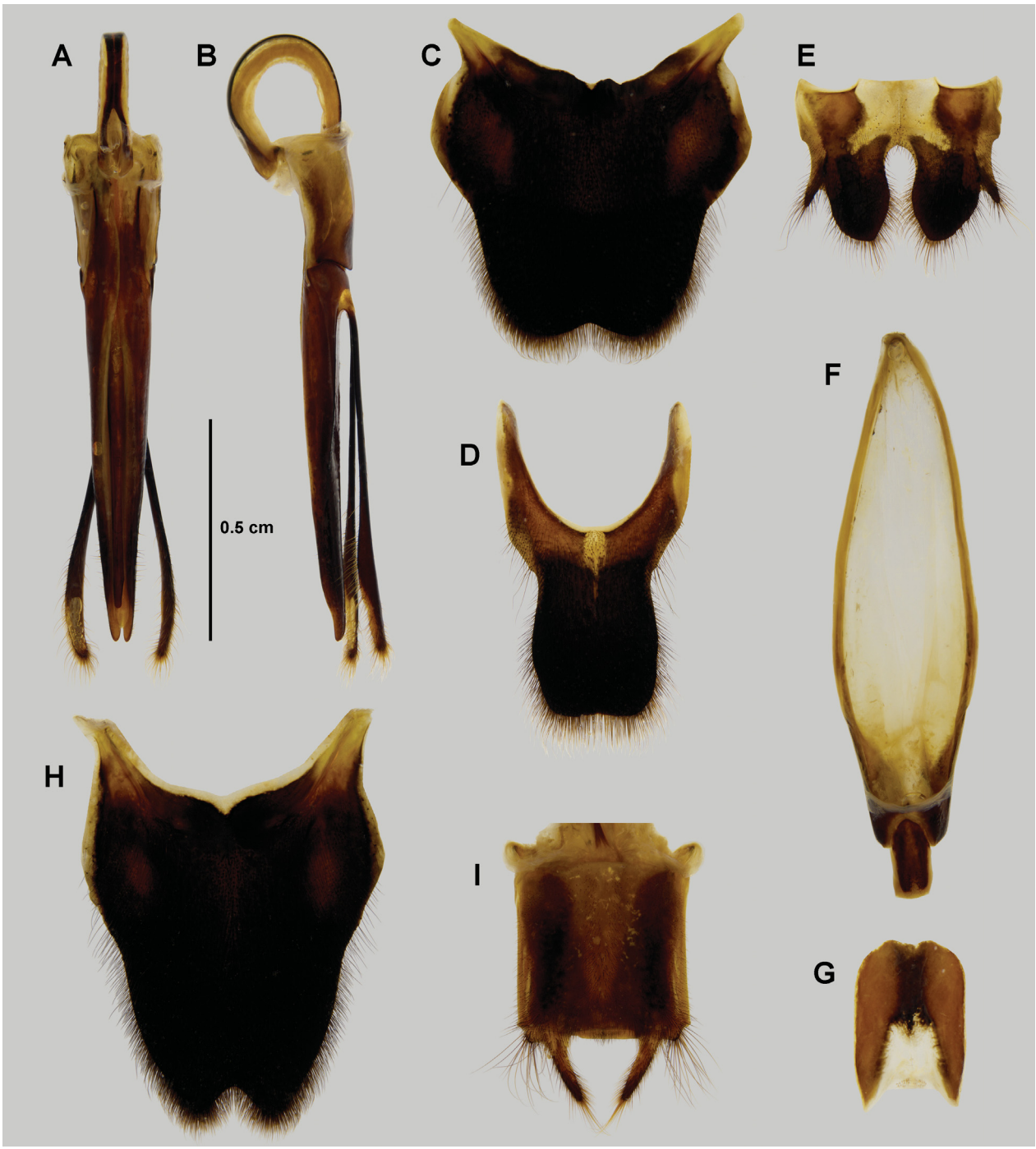

Fig. 4. Genitalia and terminalia of *Autocrates soni* sp. nov. A–B – aedeagus in dorsal and lateral views; C – male tergite VII; D – male tergite VIII; E – male sternite VIII; F–G – male tergites IX–X and detached terminal sclerite; H – female tergite VII; I – female tergite VIII and sternite VIII.

Fig. 5. Ventral view of head and thorax of *Autocrates* spp. A – *Autocrates soni* sp. nov.; B – *Autocrates vitalisi* Vuillet, 1912.

Acknowledgements

We would like to sincerely thank Tae-Wan Kim (Mancheon Insect Museum, South Korea) for providing material and type locality information of this new species. We also thank two reviewers, Rolf Georg Beutel and Fang-Shuo Hu, and the editor, Petr Kment, for their valuable comments on the manuscript. This work was supported by the Nakdonggang National Institute of Biological Resources (NNIBR) under project No. NNIBR-2024-2101.

References

ANTIL S., ABRAHAM J. S., SRIPOORNA S., MAURYA S., DAGAR J., MAKHIJA S., BHAGAT P., GUPTA R., SOOD U., LAL R. & TOTEJA R. 2023: DNA barcoding, an effective tool for species identification: a review. *Molecular Biology Reports* **50**: 761–775.

CHEN H., OLMI M., ØDEGAARD F., CAPRADOSSI L. & LIU J. 2024: DNA barcoding unveils new species of the sexually dimorphic genus *Anteon* Jurine (Hymenoptera, Dryinidae) from China. *Insects* **15 (18)**: 1–27.

CHO H.-W., KWON M. C., KIM S. K. & BEUTEL R. G. 2022: Morphology of larvae and pupae of the genus *Autocrates* (Coleoptera: Trictenotomidae) and its phylogenetic implications. *Acta Entomologica Musei Nationalis Pragae* **62**: 197–210.

HEBERT P. D., RATNASINGHAM S. & DE WAARD J. R. 2003: Barcoding animal life: cytochrome c oxidase subunit 1 divergences among closely related species. *Proceedings of the Royal Society of London Series B: Biological Sciences* **270**: S96–S99.

HU F.-S., DRUMONT A. & TELNOV D. 2022: A new *Autocrates* J. Thomson, 1860 (Coleoptera: Trictenotomidae) from Dayaoshan, S China: The importance of biodiversity refugia. *Annales Zoologici* **72**: 371–388.

LEE S., DRUMONT A., TELNOV D., LEE S. & BAI M. 2024: Molecular phylogeny of Trictenotomidae (Coleoptera: Tenebrionoidea): insights into species validation and biogeography of genus *Autocrates*. *Zoological Journal of the Linnean Society* **201 (4)**: 1–10.

MA Z., REN J. & ZHANG R. 2022: Identifying the genetic distance threshold for Entiminae (Coleoptera: Curculionidae) species delimitation via COI barcodes. *Insects* **13 (261)**: 1–12.

McKENNA D. D., SHIN S., AHRENS D., BALKE M., BEZA-BEZA C., CLARKE D. J., DONATH A., ESCALONA H. E., FRIEDRICH F., LETSCH H., LIU S., MADDISON D., MAYER C., MISOF B., MURIN P. J., NIEHUIS O., PETERS R. S., PODSIADLOWSKI L., POHL H., SCULLY E. D., YAN E. V., ZHOU X., ŚLIPIŃSKI A. & BEUTEL R. G. 2019: The evolution and genomic basis of beetle diversity. *Proceedings of the National Academy of Sciences* **116**: 24729–24737.

MEIER R., HARTOP E., PYLATIUK C. & SRIVATHSAN A. 2024: Towards holistic insect monitoring: species discovery, description, identification and traits for all insects. *Philosophical Transactions of the Royal Society B* **379 (20230120)**: 1–8.